Scientific Reports

https://doi.org/10.1038/s41598-026-37557-0

Article in Press

Comparative transcriptomic dynamics reveal molecular responses of susceptible and resistant *Triticum aestivum* genotypes to wheat stripe mosaic virus

Received: 3 October 2025

Accepted: 22 January 2026

Published online: 27 January 2026

Cite this article as: Nascimento S.C., Pereira F.S., Silva V.I.A. *et al.* Comparative transcriptomic dynamics reveal molecular responses of susceptible and resistant *Triticum aestivum* genotypes to wheat stripe mosaic virus. *Sci Rep* (2026). https://doi.org/10.1038/s41598-026-37557-0

Samara Campos Nascimento, Fernando Sartori Pereira, Vinicius Iura Abreu Silva, Vanucci Marcos Santi, Giselle Camargo Mendes, Douglas Lau, Antonio Nhani Junior, Poliana Fernanda Giachetto, Emilyn Emy Matsumura & Fabio Nascimento Silva

Comparative transcriptomic dynamics reveal molecular responses of susceptible and resistant *Triticum aestivum* genotypes to wheat stripe mosaic virus

Samara Campos Nascimento[1], Fernando Sartori Pereira[1], Vinicius Iura Abreu Silva[1], Vanucci Marcos Santi[1], Giselle Camargo Mendes[2,5], Douglas Lau[3], Antonio Nhani Junior[4], Poliana Fernanda Giachetto[4], Emilyn Emy Matsumura[5], Fabio Nascimento Silva[1,5*]

[1]Department of Agronomy, Laboratory of Plant Virology, Universidade do Estado de Santa Catarina, Lages, SC, 88520-000, Brazil

[2]Laboratory of Biotechnology, Instituto Federal de Santa Catarina – Campus Lages, Lages, SC, 88506-400, Brazil

[3]Embrapa Florestas, Colombo, PR, 83411-000, Brasil.

[4]Embrapa Agricultura Digital, Campinas, SP, 13083-886, Brasil.

[5]Laboratory of Virology, Wageningen University & Research, Wageningen, 6708 PB, The Netherlands.

Corresponding authors: Fabio Nascimento Silva (email: fabio.silva@udesc.br)

Douglas Lau (email: douglas.lau@embrapa.br)

ABSTRACT

Soil-borne wheat mosaic disease (SBWMD), caused by wheat stripe mosaic virus (WhSMV), poses an emerging threat to wheat production in South America. In this study, we analyzed the transcriptomic responses of two *Triticum aestivum* genotypes exhibiting contrasting resistance levels to WhSMV. The resistant cultivar, Embrapa 16, displayed low viral accumulation and either mild or no symptoms, whereas the susceptible cultivar, BRS Guamirim, exhibited pronounced chlorosis, stunting, and elevated virus titers. RNA-Seq analysis identified 13,225 differentially expressed genes (DEGs) across four

genotype-infection contrasts. In Embrapa 16, WhSMV infection resulted in the enrichment of Gene Ontology (GO) terms associated with defense responses, kinase activity, and hormone signaling, with marked induction of genes such as RPP13-like, RGA3, and shikimate kinase. In contrast, BRS Guamirim demonstrated extensive downregulation of photosynthesis-related genes and a disrupted hormonal response, indicating compromised metabolic homeostasis under stress. KEGG and Plant Reactome pathway analyses revealed the activation of MAPK signaling and plant–pathogen interaction pathways in the resistant genotype. These results suggest that effective resistance to WhSMV entails coordinated activation of signaling cascades, secondary metabolism, and chloroplast protection mechanisms, providing molecular insights to inform breeding strategies aimed at durable virus resistance in wheat.

Keywords: wheat stripe mosaic virus, benyvirus, soil-borne wheat mosaic disease, transcriptomic responses, resistance mechanisms, plant–pathogen interactions

1. Introduction

Wheat (*Triticum aestivum*) is among the most extensively cultivated cereal crops worldwide and serves as a fundamental dietary resource for a large segment of the global population [1]. Its cultivation in Brazil, especially in the subtropical region, assumes a critical role in safeguarding food security and sustaining regional economies. Nevertheless, wheat productivity and grain quality are undermined by

numerous diseases, with soil-borne wheat mosaic disease (SBWMD), caused by wheat stripe mosaic virus (WhSMV), being among the most damaging [2,3]. WhSMV, classified within the family *Benyviridae*, was confirmed as the etiological agent of SBWMD in Brazil after comprehensive investigations overturned the long-standing assumption that soil-borne wheat mosaic virus (*Virgaviridae* family) was responsible [4]. Following its identification in Brazil, WhSMV was subsequently documented in Paraguay [5] and South Africa [6].

WhSMV has a bipartite, single-stranded, positive-sense, polyadenylated RNA genome. The first segment, RNA-1, is about 6,600 nucleotides (nt) in length and encodes a single large polyprotein of 231.7 kDa. This polyprotein comprises four conserved functional domains that are indispensable for viral replication: methyltransferase, helicase, papain-like protease, and RNA-dependent RNA polymerase [4]. The second segment, RNA-2, is about 4,900 nt in length and harbor six open reading frames (ORFs), consistent with the organization of other benyvirids [4,6]. The first of these encodes the coat protein (CP), which has a molecular mass of 18.9 kDa. The second ORF is in-frame with the CP and, through an amber stop codon readthrough, translates into an extended protein referred to as the readthrough protein (RT), thought to facilitate transmission by the vector [7]. Furthermore, three overlapping ORFs together constitute the triple gene block, which encodes proteins of 54.6, 13.8, and 12.8 kDa involved in cell-to-cell viral movement. Near the 3′ end of RNA-2, the sixth ORF encode a

hypothetical 2.8 kDa protein that has been associated with gene silencing suppression activity in other benyvirids [4,6].

Wheat plants infected by WhSMV typically display symptoms including yellow mosaic patterns on leaves and stems, stunting, excessive tillering, and poorly developed root systems. The virus is transmitted through the plasmodiophorid *Polymyxa graminis*, a soil-borne vector characterized by highly resilient resting spores that complicated disease control [4,8]. Although agronomic measures as crop rotation can reduce disease incidence, the deployment of genetic resistance remains the most reliable and sustainable strategy for managing WhSMV [9].

In Brazil, the Embrapa 16© cultivar is characterized by the presence of two unknow dominant genes that confer resistance to the SBWMD-associated virus [10]. Although the exact mechanism of resistance remains unclear, resistant plants may disrupt critical stages of the viral infection cycle, such as restricting viral movement within plant tissues. Studies on American wheat cultivars suggest that resistance to SBWMV involves restricting the virus's movement from roots to aerial parts [11]. Despite these insights, significant gaps persist in our understanding of the genes and metabolic pathways underlying resistance in Brazilian cultivars. Since identification of the new causal agent associated with wheat mosaic in Brazil, no transcriptomic studies of this nature have been conducted, leaving key questions about resistance mechanisms unanswered.

RNA sequencing (RNA-Seq) has become an essential method for investigating plant pathogen interactions under diverse biotic stress conditions. This high-throughput approach generates a comprehensive overview of transcriptional activity, allowing the identification of differentially expressed genes and the regulatory pathways involved in plant defense [12]. In relation to SBWMD, RNA-Seq offers a valuable framework for dissecting the molecular basis of genetic resistance and for deepening our understanding of wheat responses to WhSMV.

In this study, we analyzed the transcriptional profiles of wheat genotypes exhibiting different levels of resistance to WhSMV. Our analysis revealed distinct gene expression patterns associated with resistance and susceptibility, underscoring the involvement of metabolic and signaling pathways in regulating the defense response against the virus. These findings contribute to the growing understanding of resistance mechanisms to WhSMV and lay the groundwork for developing more effective integrated management strategies.

2. Material and methods

2.1 *Plant Materials and Experimental Design*

Plants from the cultivar Embrapa 16 (resistant) and the cultivar BRS Guamirim (susceptible) were collected during field trials at Brazilian Agricultural Research Corporation (Embrapa Wheat), a research unit of the Brazilian Agricultural Research Corporation, located in the municipality of Passo Fundo, Rio Grande do Sul, Brazil (28°13' S, 52°24'

W, altitude 684 m). This site has a documented history of SBWMD, and sample collection took place during the 2021 wheat growing season. The plants were obtained from the field, where they experienced natural infection. The plant material was collected in the field with agreement from the Embrapa. Access to genetic resources was registered in the National System for the Management of Genetic Heritage and Associated Traditional Knowledge (SISGEN) under registration number [SISGEN-A830B09], in accordance with Law Nº. 13.123/2015.

For each cultivar, plants showing typical mosaic symptoms and asymptomatic plants were collected at the grain-filling stage (97 days after sowing) from the same experimental unit. Conventional RT-PCR and absolute RT-qPCR were then used to confirm infection status. Stems and leaf tissues from each sample were then stored at −80 °C until laboratory analysis.

Based on infection status and genotype, the experimental design included four biological conditions: Embrapa 16 non-infected (E16C), Embrapa 16 infected (E16S), BRS Guamirim non-infected (GuaC), and BRS Guamirim infected (GuaS). Each condition was represented by two independent biological replicates, totalling eight RNA-Seq libraries, each with at least three technical replicates. Each biological replicate corresponded to an individual plant collected from the same field trial and processed independently through RNA extraction, library preparation, sequencing, and downstream analyses.

2.2 *Resistance Assessment of Wheat Genotypes to WhSMV*

Total RNA was extracted from eight individual samples representing two wheat genotypes, with two biological replicates per genotype, including both WhSMV-infected and non-infected plants (indicated throughout the article with the initial "S" for symptomatic and "C" for control, respectively). For RNA extraction, 100 mg of frozen plant tissue was processed using QIAzol Lysis Reagent (Qiagen) following the manufacturer's instructions. RNA quality was assessed by agarose gel electrophoresis of 3 µg of total RNA from each sample. Total RNA samples were used for first-strand cDNA synthesis by using the M-MLV Reverse Transcriptase enzyme (Promega®) and an oligo(dT) primer (Promega®), with 1 µg of total RNA as input. The cDNA samples obtained were subjected to conventional PCR using the primer pair Ben_CP-fw (5'-TCA CCA AGT GTC GCA AGC-3') and Ben_CP-rev (5'-AGA ACT CCG CAG CTC TCA G- 3') which amplifies a 632-nucleotide fragment within the CP ORF of WhSMV. The presence or absence of the virus was confirmed by visualization of amplification products on an agarose gel. WhSMV titers were subsequently quantified by qPCR. Absolute quantification of viral copies was performed using 7500 Software v2.0.6 (ABI, Life Technologies) by determining the cycle threshold (Ct) value. Each reaction consisted of 1 µL of cDNA (200 ng/µL) in a final volume of 10 µL. The reaction mixture contained 5 µL of SYBR Green PCR Master Mix reagent (2×) (Applied Biosystems), 0.5 µL of each primer (10 µM), and 3 µL of ultrapure water. The qPCR primers, qPCR-CP F and qPCR-CP R, targeted the CP coding region and

had the following sequences: 5'-TGT GCC ATC GTG TTA GTA CC-3' and 3'-GTC AAT AAA ACC ACT CAA GAC CG-5', respectively. The PCR cycling conditions included an initial denaturation at 95 °C for 10 min, followed by 34 cycles of denaturation at 95 °C for 15 s and annealing/extension at 55°C for 60 s. WhSMV titers in each sample were calculated using a standard curve generated from serial dilutions of the target CP gene cloned into the pGEM-T Easy Vector (Promega, Madison, WI, USA,). All WhSMV-infected samples and standard controls were analyzed in triplicate, with three technical replicates per sample. The coefficient of determination and slope were obtained by plotting Ct values against the log-transformed concentrations of plasmid DNA. The number of WhSMV copies in each sample was calculated by interpolating the Ct value from the standard curve. For statistical analysis, means were compared using Tukey's ($p < 0.05$).

2.3 *High- throughput Sequencing*

The quality of the cDNA library was evaluated using the Agilent Bioanalyzer 6000 system (Santa Clara, CA, USA) with the 2100 Expert High Sensitivity DNA Assay. Final cDNA libraries were sequenced on the Illumina HiSeq 4000 platform (San Diego, CA, USA).

2.4 *Transcriptome Analysis*

Quality control filtering was initially performed by removing reads containing adapter sequences or poly-N regions, and low-quality bases were assessed using the FastQC program. High-quality clean reads

were retained and used for all subsequent analyses. *De novo* transcriptome assembly was carried out using *Trinity* (version 2.9.1), and assembly quality was evaluated by remapping the reads to the assembled transcriptome with *Bowtie2* v2.3.4.2 [13].

2.5 *Differential Expression Analysis*

A count matrix of mapped fragments was generated using RSEM to estimate transcript abundance, considering gene number and length using the Ex90N50 metric [13]. Differentially expressed genes were identified using an adjusted p-value (FDR) ≤ 0.05 and an expression change of two-fold or greater ($|\log_2 \text{FoldChange}| \geq 1$) between two contrasts. This threshold was selected to prioritize genes exhibiting biologically meaningful expression changes. Sample clustering based on expression data and principal component analysis was performed using the edgeR software package [14,15], and the corresponding quality control metrics, PCA plots, sample correlation heatmap, and volcano plots are provided in the Supplementary Material (Supplementary Dataset 1 and Figures S1–S3). Genes with $\log_2$FoldChange values < 1 were retained in the expression matrix but were not classified as DEGs and were excluded from downstream enrichment analyses.

2.6 *Functional Analysis*

To investigate the biological functions of the DEGs, we mapped them to the Gene Ontology (GO) database (http://geneontology.org/)

to examine their involvement in biological processes (BP), molecular functions (MF), and cellular components (CC). We also annotated the DEGs using the Plant Reactome (https://plantreactome.gramene.org/) and the KEGG database (http://www.genome.jp/kegg) to identify associated biological pathways. DEGs corresponding to the most represented GO terms and enriched pathways were selected for further discussion. Additionally, significantly enriched GO terms were identified using Fisher's Exact Test, with a false discovery rate threshold of 0.05. All functional annotation and enrichment analyses were conducted using the OmicsBox platform (https://www.biobam.com/omicsbox/).

2.7 Validation of Transcriptomics Data by RT-qPCR

Quantitative reverse transcription PCR (RT-qPCR) was performed using two biological replicates per genotype and three technical replicates per sample. First-strand cDNA was synthesized from 1 µg of total RNA using M-MLV Reverse Transcriptase enzyme (Promega®) and an oligo dT primer (Promega®), following the manufacturer's instructions. Specific primers for RT-qPCR were designed using NCBI Primer-BLAST (RRID: SCR_003095), with default parameter settings (see Supplementary Dataset 2). RT-qPCR was conducted on an ABI 7500 Real-Time PCR system (Applied Biosystems) using SYBR Green Master Mix reagent (2×) in 10 µL reactions. Thermal cycling conditions were as follows: 94 °C for 10 min, 45 cycles of 94 °C for 10 s, followed

by 60 °C for 10 s, and 72 °C for 10 s. Fluorescence was monitored via a melting curve analysis from 60 to 97 °C. Relative expression levels of selected genes were calculated using the $2^{-\Delta\Delta Ct}$ method (Livak and Schmittgen, 2001), with normalization to the reference genes *TubB* (accession: U76896) and *GAPDH* (accession: NM_001405844).

3 Results

3.1 Evaluation of Resistance of Wheat Genotypes to WhSMV

The resistance levels of the wheat genotypes in this study were assessed by quantifying viral accumulation via absolute RT-qPCR. The resistant genotype, Embrapa 16, exhibited mild or no detectable disease symptoms, consistent with field observations, and maintained normal growth and stature. By contrast, the susceptible genotype, BRS Guamirim, displayed pronounced symptoms, including yellow mosaic, leaf chlorosis, stunting, and growth underdevelopment (Figure 1 - A). RT-qPCR further confirmed the absence of viral RNA in control plants.

Among the infected samples, Embrapa 16 had an average viral load of approximately 4.80×10^4 copies, whereas BRS Guamirim reached significantly higher levels, averaging 1.48×10^5 copies. ANOVA revealed a significant effect of genotype on viral load among infected plants ($p = 0.0031$) (Figure 1 – B and Supplementary Dataset 3). Tukey's post-hoc test indicated that BRS Guamirim accumulated significantly higher viral titers than Embrapa 16, with a mean difference of 1.00×10^5 copies. These findings corroborate phenotypic

assessments, confirming that Embrapa 16 exhibits greater resistance to WhSMV, as evidenced by milder or no detectable disease symptoms and markedly lower virus accumulation.

3.2 Sequencing Output and Assembly

To gain a global view of transcriptomic changes in wheat in response to WhSMV infection, expression profiles of resistant and susceptible genotypes (Embrapa 16 and BRS Guamirim, respectively) were compared under infected and non-infected conditions. A total of 8 RNA-Seq libraries were generated (four treatments x two biological replicates) yielding 295,866,000 reads. Approximately 100,000 genes were identified, with an average GC content of 45.41%.

3.3 Differential Expression Analysis

Transcript read counts were quantified using fragments per kilobase per million (FPKM) normalized matrix to enable comparisons of mRNA expression levels. Differentially expressed genes (DEGs) were identified as those with an adjusted p-value (FDR) ≤ 0.05, indicating significant enrichment (up and down) in plants infected with WhSMV relative to non-infected controls. Four pairwise comparisons were established: E16C vs. E16S, GuaC vs. GuaS, E16S vs. GuaS, and E16C vs. GuaC (E16 and Gua – Embrapa 16 and BRS Guamirim genotypes, respectively; C and S – WhSMV non-infected and infected,

respectively). Following assessment of gene expression profiles, we identified a total of 13,225 DEGs across the WhSMV-infected and non-infected libraries. In the E16C vs. E16S comparison, 2,244 DEGs were detected, including 1,422 upregulated and 822 downregulated genes. Similarly, 2,505 DEGs were found in the GuaC vs. GuaS comparison (1,697 upregulated and 808 downregulated), 5,172 DEGs in the E16S vs. GuaS comparison (3,427 upregulated and 1,745 downregulated), and 3,331 DEGs in the E16C vs. GuaC comparison (2,087 upregulated and 1,244 downregulated) (Figure 2 - A). These results demonstrate that the transcriptional response to WhSMV infection differs markedly between the resistant genotype (Embrapa16) and susceptible genotype (BRS Guamirim). The resistant genotype exhibited a more balanced gene expression profile, whereas the susceptible genotype showed more extensive transcriptional reprogramming in response to viral infection. Notably, the comparison between infected genotypes (E16S vs. GuaS) yielded the highest number of DEGs, suggesting a strong genotype-specific response to WhSMV.

Additionally, a Venn diagram analysis illustrated the distribution and overlap of DEGs across the four comparison groups. A total of 94 DEGs were shared among all groups, while the E16S vs. GuaS comparison exhibited the largest group-specific DEG set, comprising 962 genes. These results highlight the distinct transcriptional changes associated with both infection status and genotype (Figure 2 - B).

To explore the biological processes modified in wheat in response to WhSMV infection, DEGs were annotated and categorized into the three GO domains using OmicsBox: BP (biological process), CC (cellular component), and MF (molecular function). A total of 7,041 GO annotations were identified across all comparisons, including both enriched and non-enriched terms (Supplementary dataset 4). Among these, 307 GO terms were significantly enriched based on Fisher's enrichment test (adjusted p-value < 0.05), comprising both overrepresented and underrepresented categories (Supplementary dataset 5). The enriched GO terms were distributed as follows: 184 in BP, 61 in CC, and 62 in MF.

In the MF category, DEGs were predominantly associated with binding activities, particularly adenyl nucleotide binding, ATP binding, ion binding, and protein kinase activity. Within the CC category a significant number of genes were related to structural components such as membrane, integral components of membrane, cytoplasm, and nucleus. For the BP category, highly represented terms included metabolic processes, oxidation–reduction process, response to stress, signal transduction, and cellular response to stimulus (Figure 3).

Fisher's enrichment analysis of GO terms offered valuable insights into the biological functions of DEGs across multiple comparisons. In this study, we focus on the E16C vs E16S and GuaC vs GuaS comparisons, as both include a control without virus infection. In the E16C vs E16S the most significantly enriched GO terms included

metabolic processes, protein kinase activity, and defense responses, as illustrated in Figure 4 – (1). Among the DEGs upregulated in symptomatic plants, enriched GO terms comprised kinase activity (GO:0004672), including protein kinase activity and phosphotransferase activity (GO:0016773) as well as nucleotide binding and defense response (GO:0006952) (Figure 4). These findings suggest activation of signaling and defense pathways in response to viral infection. Conversely, DEGs upregulated in the control conditions were enriched in broader categories such as metabolic processes (GO:0008152), macromolecule biosynthesis (GO:0009059), transmembrane transport (GO:0055085), and catalytic activity (GO:0003824). Additionally, enriched GO terms related to cellular components including intracellular organelles (GO:0043229), cytoplasm (GO:0005737), and plasma membrane (GO:0005886) indicate that viral infection influences cellular organization and metabolic activity (Figure 4).

In the GuaC vs GuaS comparison, notably, enriched terms among down-regulated genes included nucleic acid binding (GO:0003676), RNA binding (GO:0003723), and zinc ion binding (GO:0008270), as well as key components involved in photosynthetic processes, such as photosynthesis (GO:0015979), DNA-templated transcription (GO:0006351), and nucleus (GO:0005634). Conversely, among the upregulated genes, enriched GO terms encompassed hydrolase activity (GO:0016787), serine-type peptidase activity (GO:0008236), cell recognition (GO:0008037), and several plastid-associated

components such as thylakoid membrane (GO:0042651) and plastid envelope (GO:0009526) (Figure 4 – (2)).

The results indicate that WhSMV infection elicits distinct biological responses in resistant and susceptible wheat genotypes. In the resistant genotype, Embrapa 16, the enriched GO terms highlighted the activation of defense mechanisms and stress-related pathways. In contrast, the susceptible genotype BRS Guamirim exhibited an increased activity in processes related to photosynthesis and nucleic acid binding, suggesting a greater disruption of metabolic functions caused by viral infection.

3.4 Metabolic Pathway Analysis for DEGs in the Tested Genotypes

To investigate the molecular mechanisms underlying resistance and susceptibility to WhSMV, DEGs were mapped onto metabolic pathways using the KEGG and Plant Reactome databases. In the E16C vs E16S comparison, KEGG analysis revealed significant enrichment in the plant–pathogen interaction pathway (ko04626), comprising key immune-related genes such as *PR1* (Pathogenesis-Related Protein 1), *WRKY33* (WRKY transcription factor 33), Disease resistance protein *RPM1*, *NBS-LRR* (Nucleotide-Binding Site – Leucine-Rich Repeat proteins), *CML16* (Calmodulin-Like Protein 16), and protein kinases (Figure 5). Additionally, although with marginal statistical significance, the plant MAPK signaling pathway (ko04016) was also identified, reinforcing the involvement of kinase cascades in antiviral defense. Supporting these findings, the Plant Reactome analysis identified

salicylic acid signaling (R-ATA-6788019) as significantly enriched (adj. p = 0.003), emphasizing the hormonal regulation of defense responses (Figure 6 - A).

In contrast, the GuaC vs GuaS comparison reflecting the susceptible genotype (BRS Guamirim) demonstrated considerably weaker activation of defense-related pathways (Figure 6 - B). While no statistically significant enrichment was observed in canonical immune pathways in KEGG, the Plant Reactome analysis identified only polyisoprenoid biosynthesis as enriched a pathway associated with membrane lipid metabolism rather than immune response. Furthermore, several pathways involved in secondary metabolite biosynthesis and hormone signaling, such as trans-zeatin and coumarin biosynthesis, were downregulated, suggesting suppression or dysregulation of defense-associated metabolic branches. Notably, the pathway for recognition of fungal and bacterial pathogens and immunity response was underrepresented, reinforcing the hypothesis of a weakened or inadequate immune activation in BRS Guamirim during WhSMV infection (Figure 6 - B).

Together, these findings underscore a fundamental contrast between genotypes. Embrapa 16 exhibited an active and coordinated defense strategy involving pathogen recognition, kinase signaling, and hormonal activation, particularly through salicylic acid. In contrast, BRS Guamirim failed to activate key defense pathways, instead showing evidence of suppression in immune- and hormone-related responses.

This divergence at the pathway level likely contributes to the differential viral accumulation and symptom expression observed between resistant and susceptible genotypes.

3.5 Validation of the Differentially Expressed Transcripts (DETs) by RT-qPCR Analysis

To evaluate the reliability and biological consistency of the transcriptome dataset, twenty-one DETs related to defense responses were selected for validation via RT-qPCR (Supplementary Dataset 2). The results confirmed the expression trends observed in the RNA-Seq analysis (Supplementary dataset 4 and 5, Supplementary Figure S4). Among the validated genes, shikimate kinase, putative disease resistance protein *RPP13-like*, and *RGA3* were significantly upregulated in WhSMV-infected tissues of the resistant genotype (Embrapa 16) but were not induced in the susceptible cultivar (BRS Guamirim), suggesting their involvement in resistance-related pathways (Figure 7). In contrast, *CML16*, a calmodulin-like calcium-binding protein, was upregulated in response to WhSMV in both genotypes, as confirmed by RNA-Seq. Notably, the strongest induction occurred in the resistant genotype, indicating that calcium signaling is broadly activated during viral infection. This emphasizes the importance not only of initiating signaling cascades but also of integrating them with downstream immune responses. Overall, the RT-qPCR results aligned with the RNA-

Seq expression profiles, supporting the robustness of the transcriptomic analysis.

4 Discussion

In this study, we analyzed the transcriptional responses of wheat genotypes with contrasting resistance to WhSMV, the causal agent of SBWMD in Brazil. Resistance or susceptibility was validated through visual inspection of disease symptoms and quantification of viral RNA using RT-qPCR. The resistant genotype, Embrapa 16, showed minimal or no visible symptoms and maintained low viral titers, whereas the susceptible cultivar, BRS Guamirim, displayed typical symptoms including yellow mosaic, stunting, and reduced root growth accompanied by high levels of viral accumulation. These findings are consistent with the classical model of resistance described by Cooper and Jones [16], in which resistant hosts limit viral replication, thereby constraining both virus accumulation and symptom development. Nonetheless, field studies by Pereira et al.[17], under natural field infection in the wheat–WhSMV pathosystem, demonstrated that this relationship can be more complex. Their data showed that in some years (e.g., 2021) higher viral loads were correlated with more severe symptoms in susceptible cultivars, whereas in others (e.g., 2022), resistant or moderately resistant cultivars accumulated higher viral titers than susceptible ones but displayed only mild or nearly imperceptible symptoms. This emphasizes the multifaceted nature of

plant–virus interactions and corroborates the earlier observations of Comeau and Haber [18], who argued that resistance cannot be defined solely by viral concentrations but must also account for the plant's ability to restrict viral replication and systemic movement. These results underscore the importance of evaluating not only visible symptoms and viral titers but also the molecular responses that determine such contrasting outcomes.

Here, RNA-Seq analysis was undertaken to characterize the transcriptional profiles associated with WhSMV infection, with the aim of elucidating how gene expression patterns contribute to the phenotypic divergence between resistant and susceptible genotypes.

RNA-Seq analysis revealed distinct transcriptional profiles between genotypes and infection conditions, providing insights into the molecular mechanisms underlying resistance. A total of 13,225 DEGs were identified across all libraries, with the highest number found in the E16S vs. GuaS comparison (5,172 DEGs), reflecting a pronounced contrast between resistant and susceptible genotypes under viral stress. The comparisons E16C vs. E16S and GuaC vs. GuaS revealed 2,244 and 2,505 DEGs, respectively, further supporting genotype-specific responses to WhSMV.

GO enrichment analysis classified the DEGs into 184 BP, 61 CC, and 62 MF. In the E16C vs E16S comparison, the upregulated DEGs in symptomatic plants were primarily associated with kinase activity (GO:0004672), phosphotransferase activity (GO:0016773), nucleotide

binding, and defense responses (GO:0006952), suggesting that signaling pathways are activated in response to WhSMV infection. These findings are consistent with those of Fontes et al. (2021) [19], who emphasized the crucial role of receptor-like kinases and subsequent phosphorylation cascades in orchestrating antiviral defenses, as well as their crosstalk with other immune pathways. Similarly, Sharaf et al. [20] demonstrated that virus infection in wheat, caused by a geminivirus (wheat dwarf virus, WDV, *Mastrevirus hordei*), leads to significant transcriptional reprogramming, accompanied by GO enrichment in kinase- and defense-related processes. In contrast, DEGs upregulated in control plants (i.e., uninfected) in our dataset were enriched in primary metabolic processes (GO:0008152), macromolecule biosynthesis (GO:0009059), and transmembrane transport (GO:0055085).

In the comparison between GuaC and GuaS, enriched GO terms included photosynthesis (GO:0015979), nucleic acid binding (GO:0003676), and serine-type peptidase activity (GO:0008236). Notably, genes involved in photosynthesis, such as *psbP-like* proteins and components of the chloroplast reaction center were significantly downregulated in infected tissues. These tissues exhibiting typical symptoms, including yellow mosaic, stunting, and root reduction, hallmark manifestations commonly observed in plant–virus interactions [21]. The ability of viruses to manipulate chloroplast structure and function is crucial for the viral infection cycle. Zhao et al. [21] demonstrated that viruses can alter the expression of chloroplast

photosynthesis-related genes, disrupt ultrastructural features such as thylakoid membranes and grana stacks, and interfere with the assembly of photosystems I and II. These findings are consistent with transcriptome analyses of wheat infected with WDV, which also revealed enriched GO terms related to photosynthesis, phytohormone signaling, and immune responses. This reinforces the central role of chloroplast-associated processes in symptom development during viral infection [12,22]. Such alterations not only reduce photosynthetic efficiency but also impair chloroplast-mediated signaling, a critical for activating defense responses. In contrast, in Embrapa 16, the same photosynthesis-related genes were either maintained or upregulated following WhSMV infection, indicating a potential protective mechanism that sustains chloroplast integrity and functionality under viral stress. This preservation may buffer against typical energy imbalance and oxidative stress, phenomena typically exacerbated during infection, thereby contributing to milder symptom expression and greater photosynthetic stability, an effect previously proposed for resistant wheat genotypes [12,20]. These observations prompted further investigation into genes directly associated with chloroplast homeostasis and hormone signaling in both genotypes.

Moreover, our detailed examination of chloroplast- and hormone-related genes offers further insight into the molecular basis underlying the differential symptom severity observed between the genotypes. In BRS Guamirim, a broader set of chloroplast-associated genes, including those encoding key components of the photosynthetic apparatus, such

as PSI reaction center subunit VI, chloroplastic chaperones, and 6-phosphogluconolactonase, were significantly downregulated upon WhSMV infection, indicating a more severe disruption of photosynthetic processes. This trend aligns with studies reporting that viruses commonly suppress chloroplast-related genes to facilitate their replication and movement, thereby intensifying chlorosis and promoting energy imbalance [23,24.] Simultaneously, BRS Guamirim exhibited a dysregulated hormonal transcriptional profile, with auxin- and ethylene-responsive isoforms showing both up- and downregulation under viral stress. Such conflicting hormonal responses are known to impair defense signaling and amplify symptom expression, as viruses often exploit hormonal crosstalk to enhance infection success [25]. This observation is consistent with the findings of Alazem and Lin[25], who demonstrated that viruses can manipulate hormone signaling, particularly pathways involving auxin and ethylene, to weaken plant immunity and promote pathogenesis. Our results in BRS Guamirim reflect this mechanism. Similarly, Lv et al.[26] reported widespread disruption of hormone-related gene expression in susceptible wheat cultivars infected with stripe rust, suggesting that hormonal imbalance may be a general feature of vulnerability to diverse pathogens. By contrast, although Embrapa 16 also exhibited modulation of chloroplast and hormone-related genes, notably ethylene-responsive factors and auxin transporters, the overall number of downregulated plastidial genes was lower, and the hormonal response appeared more balanced. Notably, compensatory

upregulation of specific auxin-related genes in symptomatic tissues may help sustain growth and delay symptom progression [27,28]. These findings agree with transcriptomic studies in wheat infected by WDV, where Liu et al.[12] showed that virus-induced repression of photosynthetic genes and hormone biosynthesis pathways was closely linked to symptom expression, including chlorosis and stunting. Altogether, our results support a model in which the combined effect of extensive photosynthetic suppression and hormonal dysregulation underlies the heightened susceptibility and more severe symptoms observed in BRS Guamirim relative to Embrapa 16.

Consistent with the GO results, KEGG and Plant Reactome pathway mapping further highlighted the activation of immune responses in infected tissues. Notably, the plant–pathogen interaction pathway (map04626, as shown in Figure 6) was specifically enriched in symptomatic samples. This pathway included several classical defense-related genes, such as *PR1*, *WRKY33*, *RPM1*, *NBS-LRR*, and *CML16*, all associated with pathogen recognition, signal transduction, and immune activation [19]. Genes encoding NBS-LRR-type proteins are well known for mediating effector-triggered immunity (ETI), a robust defense mechanism in plants against biotrophic pathogens [29]. This enrichment was further supported by RT-qPCR validation, which confirmed the expression patterns of selected DEGs. In Embrapa 16, WhSMV infection led to strong upregulation of shikimate kinase, putative disease resistance protein *RPP13-like*, and *RGA3*, whereas these genes were not induced in BRS Guamirim. Shikimate kinase, a

key enzyme in the shikimate pathway, catalyzes the formation of shikimate-3-phosphate, a precursor of aromatic amino acids and phenolic compounds, including flavonoids and coumarins. Its upregulation in Embrapa 16 suggests enhanced activation of secondary metabolic pathways and potential antiviral roles of phenolic compounds. Flavonoids are recognized as multifunctional secondary metabolites that play important roles in plant defense. According to Treutter [30], they can exist in two forms: as “preformed” compounds, which are synthesized during normal tissue development and are often located in strategic areas, or as “inducible compounds”, which are produced *de novo* in response to infection or stress and act as phytoalexins. There is considerable evidence of the involvement of flavonoids in plant-pathogen interactions. Most often, this involves cross-linking of microbial enzymes, inhibition of cell wall-degrading enzymes such as cellulases, xylanases, and pectinases, chelation of metals essential for pathogen activity, or even the formation of rigid physical barriers that limit pathogen colonization. These mechanisms were found to be active in barley when attacked by *Fusarium* species, through the activation and production of proanthocyanidins and dihydroquercetin [31]. Furthermore, flavonoid accumulation has been observed at infection sites, often occurring in conjunction with hypersensitive responses and programmed cell death [30,32]. Recent work by Chen et al. [33] supports this interpretation, demonstrating that wheat cultivars resistant to *Fusarium* head blight activate detoxification pathways and reinforce cell wall structures. Likewise, the

induction of the shikimate pathway observed in our study aligns with the findings of Naoumkina et al. [32], who highlighted that phenylpropanoid-derived metabolites play central roles in antiviral plant defense. They reported that coumarins such as scopoletin and its glucoside scopolin, both derived from the shikimate–phenylpropanoid pathway, can restrict tobacco mosaic virus (TMV) infection. Exogenous application of scopoletin inhibited TMV replication in tobacco protoplasts, whereas plants with reduced scopolin/scopoletin levels showed enhanced oxidative stress and increased susceptibility to TMV [34]. Complementarily, Matros and Mock [35] reported that transgenic tobacco plants accumulating higher levels of scopoletin showed enhanced resistance to *Potato virus* Y (PVY). These findings provide direct evidence that shikimate-derived phenylpropanoids can contribute to antiviral defense, supporting the interpretation that the activation of this pathway in Embrapa 16 may enhance the production of protective metabolites, thus contributing to its superior resistance to WhSMV. Together, these findings reinforce the idea that resistance to WhSMV is not only mediated by recognition and signaling events (e.g., NBS-LRR proteins and MAPK cascades), but also by metabolic reprogramming towards phenylpropanoid-derived metabolites. Meanwhile, RPP13-like and RGA3, both encoding NBS-LRR resistance proteins, were upregulated exclusively in the resistant genotype, consistent with their established role in (ETI) [20]. This upregulation supports the ETI model proposed by Cui et al. [29] wherein NBS-LRR

proteins play a central role in recognizing pathogen effectors and initiating robust immune responses [36].

Interestingly, although both Embrapa 16 and BRS Guamirim modulated calcium-related genes during infection, only Embrapa 16 exhibited isoforms specifically induced in symptomatic tissues. This suggests that while WhSMV broadly affects calcium signaling in wheat, precise regulation of this pathway, alongside activation of ETI and flavonoid biosynthesis, may be critical components underlying the enhanced resistance observed in Embrapa 16. Notably, the consistent upregulation of *CML16* in both genotypes, and particularly in Embrapa 16, indicates that calcium signaling may serve as a promising regulatory hub for future strategies targeting virus resistance pathways.

Calcium (Ca^{2+}) is a ubiquitous second messenger in plant immunity, generating distinct spatial and temporal “signatures” that are decoded by specialized sensors such as calmodulins (*CaMs*), calmodulin-like proteins (*CMLs*), calcium-dependent protein kinases (CDPKs), and calcineurin B-like proteins (*CBLs*). These proteins affect Ca^{2+} fluctuations into immune outputs by modulating transcription factors, metabolic enzymes, and defense-associated proteins [37]. In plant–virus pathosystems, for example, the calmodulin-related protein rgsCaM (*regulator of gene silencing calmodulin*) interacts with the viral suppressor HC-Pro (*helper component–proteinase*) of tobacco etch virus (TEV), thereby modulating RNA silencing, a central antiviral

mechanism. Moreover, Ca^{2+}-dependent regulation of transcription factors such as *CBP60g* (*calmodulin-binding protein 60-like g*) and *CAMTA3* (*calmodulin-binding transcription activator 3*) influences salicylic acid (SA) biosynthesis, directly linking calcium signaling to SA-mediated defense. Beyond SA, Ca^{2+} signaling also integrates with reactive oxygen species (ROS) production via NADPH oxidases, nitric oxide (NO) bursts, and hormonal pathways including jasmonic acid (JA) and ethylene, highlighting its role as a central hub in multilayered immunity [37].

Recent findings further demonstrate that Ca^{2+}-regulated proteins are direct targets of viral effectors. Fontes et al.[19] showed that the C4 protein of geminiviruses binds to the chloroplast calcium-sensing receptor (*CAS*), thereby suppressing Ca^{2}-dependent SA defenses. In contrast, the host kinase *CPK16* relocates from the plasma membrane to the chloroplasts upon pathogen challenge, where it functions as a positive regulator of defense. Transgenic plants engineered to retain *CPK16* in chloroplasts display enhanced resistance to both viral and bacterial pathogens. In addition, several viral proteins manipulate downstream processes inherently dependent on Ca^{2+} influx. The movement protein (MP) of cucumber mosaic virus (CMV, *Cucumovirus CMV*) suppresses pathogen-associated molecular pattern (PAMP)-triggered ROS bursts [38]. The multifunctional P6 protein of cauliflower mosaic virus (CaMV) inhibits SA accumulation and SA-dependent autophagy through activation of the TOR (*target of rapamycin*) kinase [39]. The C4 protein of tomato yellow leaf curl virus (TYLCV, *Begomovirus*

coheni) interacts with multiple receptor-like kinases (RLKs), disrupting pattern-recognition receptor (PRR)-mediated signaling and hormone-associated defense pathways [40]. Complementarily, receptor-like kinases such as NIK1 (*nuclear shuttle protein-interacting kinase 1*) mediate antiviral immunity by phosphorylating ribosomal protein L10 (RPL10), which translocates to the nucleus to repress genes of the translational machinery, thereby restricting viral mRNA translation [41]. Although these viral proteins act through diverse mechanisms, they converge on signaling modules in which Ca^{2+} influx and decoding play a pivotal role, linking pathogen perception with ROS production, hormonal regulation, and translational control. Together, these findings emphasize that Ca^{2+} signaling is not only a pivotal integrator of PTI and ETI but also a critical target of viral suppressors. The selective induction of CML16 in Embrapa 16, therefore, likely reflects a fine-tuned capacity to decode Ca^{2+} signatures, reinforcing multiple defense layers—potentially including SA signaling, ROS bursts, and translation control—and ultimately contributing to its enhanced resistance to WhSMV.

Supporting this model, Wu et al. [42] demonstrated that the wheat resistance gene Yr10 confers durable protection against stripe rust by integrating SA signaling, reactive oxygen species (ROS) generation, and preservation of photosynthetic function. Although Yr10 is primarily associated with fungal resistance, it encodes a typical *NBS-LRR* protein —similar to *RGA3* and *RPP13-like*— underscoring a shared defense strategy against diverse classes of pathogens. This reinforces the notion that NBS-LRR-mediated resistance not only activates immune

responses but also contributes to maintaining metabolic stability under biotic stress. In parallel, the strong repression of photosynthesis-related genes observed in BRS Guamirim parallels the findings of Zhao et al. [21] who reported that viruses can alter chloroplast structure and function to suppress ROS-mediated signaling and facilitate viral replication. These insights could inform marker-assisted selection or gene editing strategies aimed at incorporating key resistance determinants such as NBS-LRR genes or regulators of secondary metabolism into elite wheat.

Beyond individual defense genes, our pathway-level analyses revealed that resistance in Embrapa 16 also involves extensive reprogramming of secondary metabolism and precise regulation of multiple signaling cascades. KEGG enrichment analysis highlighted significant activation of the MAPK signaling pathway (map04016), hormone signal transduction (map04075), and the plant–pathogen interaction pathway (map04626). Complementary GO categories, including protein kinase activity (GO:0004672), phosphotransferase activity (GO:0016773), and kinase activity (GO:0016301), underscored the widespread engagement of phosphorylation-dependent regulatory networks. These results suggest that Embrapa 16 likely employs a multifaceted defense strategy that involves metabolic reprogramming, chloroplasts protection, MAPK and hormonal signaling, and the expression of resistance-related genes. This aligns with transcriptomic studies in cereals, showing that resistance is typically associated with rapid and coordinated gene expression changes, whereas susceptibility

often reflects delayed or dysregulated responses [43–45]. While this study focused on transcriptomic responses, future work integrating proteomic and metabolomic analyses could further elucidate post-transcriptional regulatory mechanisms and defense responses at the metabolite level.

Comparable transcriptomic studies have been reported for other members of the family *Benyviridae*, most notably beet necrotic yellow vein virus (BNYVV) and beet soil-borne mosaic virus (BSBMV) in sugar beet and experimental hosts. In sugar beet, RNA-Seq analyses revealed extensive transcriptional reprogramming, including the activation of defense-related transcription factors and PR proteins, enrichment of SA and JA signaling pathways, and a suppression of ethylene-responsive genes, alongside modulation of auxin metabolism associated with root development [46]. In *Beta macrocarpa*, BNYVV infection induced genes linked to biotic stress responses, oxidative processes, and primary metabolism [47]. Similarly, in *Nicotiana benthamiana*, BNYVV altered the expression of more than 3,000 transcripts, including those associated with RNA silencing, the ubiquitin–proteasome system, and cell wall biosynthesis, reflecting broad manipulation of host defense and metabolic networks [48].

Several of these trends are similar to responses observed in wheat infected by WhSMV. For example, the enrichment of SA-related signaling and activation of *NBS-LRR* resistance genes in Embrapa 16 resemble the SA- and JA-mediated defense pathways reported in sugar

beet challenged with BNYVV/BSBMV. Likewise, the repression of photosynthesis- and hormone-related processes in the susceptible genotype BRS Guamirim reflects the metabolic disruption and hormonal imbalance also described in susceptible beet cultivars. Moreover, the induction of calcium-binding proteins (e.g., *CML16*) and secondary metabolism in Embrapa 16 is supported by the broader activation of signaling hubs and oxidative stress responses reported in alternative hosts of BNYVV. Collectively, these comparisons suggest that, despite differences in host species and symptomatology, members of *Benyviridae* share a common infection strategy characterized by simultaneous activation and subversion of host defense networks. To our knowledge, however, the present study is the first transcriptomic analysis of wheat responses to WhSMV, providing novel insights into the molecular basis of resistance to soil-borne viruses in cereals and expanding our understanding of host–*Benyviridae* interactions.

5 Conclusion

This study provides a comprehensive transcriptomic perspective on wheat responses to WhSMV infection by comparing a resistant (Embrapa 16) and a susceptible (BRS Guamirim) genotype. Our analyses indicated that resistance is associated with a complex defense architecture involving activation of kinase cascades, MAPK and hormone signaling, secondary metabolism, and *NBS-LRR*-mediated

effector-triggered immunity. In contrast, susceptibility appears to correlate with the extensive repression of chloroplast-associated genes and a dysregulated hormonal network, potentially exacerbating symptom severity through impaired photosynthesis and uncoordinated defense responses. These findings reinforce the idea that durable resistance to viruses in wheat depends not only on restricting viral replication but also on sustaining primary metabolic processes and preventing hormonal homeostasis under stress. Future research that integrates functional genomics, targeted gene editing, and metabolic profiling will be crucial for clarifying the interplay among these mechanisms and for directing breeding strategies aimed at improving WhSMV resistance.

REFERÊNCIAS

1. Food and Agriculture Organization of the United Nations. FAOSTAT Statistical Database. *FAO* (2024).
2. Douglas Lau. *Mosaico do Trigo*. *Fundação Pró-sementes* (2023).
3. Mar, T. B., Lau, D., Silva, F. N. da, Alemandri, V. & Pereira, P. R. V. D. S. in *Viral Diseases of Field and Horticultural Crops* 35–47 (Elsevier, 2024). doi:10.1016/B978-0-323-90899-3.00042-2
4. Valente, J. B. *et al.* A novel putative member of the family Benyviridae is associated with soilborne wheat mosaic disease in Brazil. *Plant Pathol* **68,** 588–600 (2019).
5. Esquivel-Fariña, A., Camelo-García, V. M., Kitajima, E. W., Rezende, J. A. M. & González-Segnana, L. R. First report of wheat stripe mosaic virus in Paraguay. *Australas Plant Dis Notes* **14,** (2019).
6. Gilmer, D. & Ratti, C. ICTV virus taxonomy profile: Benyviridae. *Journal of General Virology* **98,** 1571–1572 (2017).

7. Tamada, T. & Kondo, H. Biological and genetic diversity of plasmodiophorid-transmitted viruses and their vectors. *Journal of General Plant Pathology* **79,** 307–320 Preprint at https://doi.org/10.1007/s10327-013-0457-3 (2013)

8. Kanyuka, K., Ward, E. & Adams, M. J. Polymyxa graminis and the cereal viruses it transmits: A research challenge. *Mol Plant Pathol* **4,** 393–406 Preprint at https://doi.org/10.1046/j.1364-3703.2003.00177.x (2003)

9. Stempkowski, L. A. *et al.* Management of wheat stripe mosaic virus by crop rotation. *Eur J Plant Pathol* **158,** 349–361 (2020).

10. Barbosa, M. M., Goulart, L. R., Prestes, A. M. & Juliatti, F. C. *Genetic control of resistance to soilborne wheat mosaic virus in Brazilian cultivars of Triticum aestivum L. Thell*. *Euphytica* **122,** (2001).

11. Myers LD, Sherwood JL, Siegerist WC & Hunger RM. Temperature-influenced virus movement in expression of resistance to soil-borne wheat mosaic virus in hard red winter wheat (Triticum aestivum). *Phytopathology* **83,** 548–551 (1993).

12. Liu, Y., Liu, Y., Spetz, C., Li, L. & Wang, X. Comparative transcriptome analysis in Triticum aestivum infecting wheat dwarf virus reveals the effects of viral infection on phytohormone and photosynthesis metabolism pathways. *Phytopathology Research* **2,** (2020).

13. Langmead, B. & Salzberg, S. L. Fast gapped-read alignment with Bowtie 2. *Nat Methods* **9,** 357–359 (2012).

14. Yeung, K. Y. & Ruzzo, W. L. *Principal component analysis for clustering gene expression data*. *BIOINFORMATICS* **17,** (2001).

15. McCarthy, D. J., Chen, Y. & Smyth, G. K. Differential expression analysis of multifactor RNA-Seq experiments with respect to biological variation. *Nucleic Acids Res* **40,** 4288–4297 (2012).

16. Cooper, J. I. & Jones, A. T. *Letter to the Editor Responses of Plants to Viruses: Proposals for the Use of Terms*.

17. Pereira, F. S. *et al.* Resistance to wheat stripe mosaic virus (WhSMV): response of contrasting wheat genotypes under infection in the field. *Trop Plant Pathol* **49,** 322–329 (2024).

18. Comeau, A. & Haber, S. *Breeding for BYDV tolerance in wheat as a basis for multiple stress tolerance strategy Agriculture and*

Agri-Food Canada (NOT Ottawa). (2002). at <https://www.researchgate.net/publication/236232363>

19. Fontes, E. P. B., Teixeira, R. M. & Lozano-Durán, R. Plant virus-interactions: unraveling novel defense mechanisms under immune-suppressing pressure. *Curr Opin Biotechnol* **70,** 108–114 Preprint at https://doi.org/10.1016/j.copbio.2021.03.007 (2021)

20. Sharaf, A. *et al.* Transcriptome Dynamics in Triticum aestivum Genotypes Associated with Resistance against the Wheat Dwarf Virus. *Viruses* **15,** (2023).

21. Zhao, J., Zhang, X., Hong, Y. & Liu, Y. Chloroplast in plant-virus interaction. *Front Microbiol* **7,** Preprint at https://doi.org/10.3389/fmicb.2016.01565 (2016)

22. Mochizuki, T., Ogata, Y., Hirata, Y. & Ohki, S. T. Quantitative transcriptional changes associated with chlorosis severity in mosaic leaves of tobacco plants infected with cucumber mosaic virus. *Mol Plant Pathol* **15,** 242–254 (2014).

23. Bhattacharyya, D. & Chakraborty, S. Chloroplast: the Trojan horse in plant–virus interaction. *Mol Plant Pathol* **19,** 504–518 Preprint at https://doi.org/10.1111/mpp.12533 (2018)

24. Shahriari, A. G. *et al.* The crucial role of mitochondrial/chloroplast-related genes in viral genome replication and host defense: integrative systems biology analysis in plant-virus interaction. *Front Microbiol* **16,** (2025).

25. Alazem, M. & Lin, N. S. Roles of plant hormones in the regulation of host-virus interactions. *Mol Plant Pathol* **16,** 529–540 Preprint at https://doi.org/10.1111/mpp.12204 (2015)

26. Lv, X. *et al.* Comparative transcriptomic insights into molecular mechanisms of the susceptibility wheat variety MX169 response to Puccinia striiformis f. sp. tritici (Pst) infection. *Microbiol Spectr* **12,** (2024).

27. Alazem, M. & Lin, N. S. Roles of plant hormones in the regulation of host-virus interactions. *Mol Plant Pathol* **16,** 529–540 Preprint at https://doi.org/10.1111/mpp.12204 (2015)

28. Islam, W., Naveed, H., Zaynab, M., Huang, Z. & Chen, H. Y. H. Plant defense against virus diseases; growth hormones in highlights. *Plant Signal Behav* **14,** Preprint at https://doi.org/10.1080/15592324.2019.1596719 (2019)

29. Cui, H., Tsuda, K. & Parker, J. E. Effector-triggered immunity: From pathogen perception to robust defense. *Annu Rev Plant Biol* **66,** 487–511 (2015).

30. Treutter, D. Significance of flavonoids in plant resistance and enhancement of their biosynthesis. *Plant Biol* **7,** 581–591 Preprint at https://doi.org/10.1055/s-2005-873009 (2005)

31. Skadhauge, B., Thomsen, K. K. & Von Wettstein, D. The role of the barley testa layer and its flavonoid content in resistance to Fusarium infections. *Hereditas* **126,** 147–160 (1997).

32. Naoumkina, M. A. *et al.* Genome-wide analysis of phenylpropanoid defence pathways. *Mol Plant Pathol* **11,** 829–846 Preprint at https://doi.org/10.1111/j.1364-3703.2010.00648.x (2010)

33. Chen, C. *et al.* Comparative transcriptomic analysis of wheat cultivars differing in their resistance to Fusarium head blight infection during grain-filling stages reveals unique defense mechanisms at play. *BMC Plant Biol* **23,** (2023).

34. Chong, J. *et al.* Downregulation of a pathogen-responsive tobacco UDP-Glc:phenylpropanoid glucosyltransferase reduces scopoletin glucoside accumulation, enhances oxidative stress, and weakens virus resistance. *Plant Cell* **14,** 1093–1107 (2002).

35. Matros, A. & Mock, H.-P. *Ectopic Expression of a UDP-Glucose:phenylpropanoid Glucosyltransferase Leads to Increased Resistance of Transgenic Tobacco Plants Against Infection with Potato Virus Y*. *Plant Cell Physiol* **45,** (2004).

36. Wang, H. *et al.* Comparative transcriptomes reveal insights into different host responses associated with Fusarium head blight resistance in wheat. *BMC Plant Biol* **25,** (2025).

37. DeFalco, T. A., Bender, K. W. & Snedden, W. A. Breaking the code: Ca2+ sensors in plant signalling. *Biochemical Journal* **425,** 27–40 Preprint at https://doi.org/10.1042/BJ20091147 (2010)

38. Kong, J. *et al.* The cucumber mosaic virus movement protein suppresses PAMP-triggered immune responses in Arabidopsis and tobacco. *Biochem Biophys Res Commun* **498,** 395–401 (2018).

39. Zvereva, A. S. *et al.* Viral protein suppresses oxidative burst and salicylic acid-dependent autophagy and facilitates bacterial

growth on virus-infected plants. *New Phytologist* **211,** 1020–1034 (2016).

40. Garnelo Gómez, B. *et al.* The C4 Protein from Tomato Yellow Leaf Curl Virus Can Broadly Interact with Plant Receptor-Like Kinases. *Viruses* **11,** 1009 (2019).

41. Teixeira, R. M. *et al.* Virus perception at the cell surface: revisiting the roles of receptor-like kinases as viral pattern recognition receptors. *Mol Plant Pathol* **20,** 1196–1202 Preprint at https://doi.org/10.1111/mpp.12816 (2019)

42. Wu, Z. *et al.* Transcriptomic analysis of wheat reveals possible resistance mechanism mediated by Yr10 to stripe rust. *Stress Biology* **3,** (2023).

43. Zainy, Z. *et al.* Comparative transcriptome analysis of resistant, moderately resistant, and susceptible wheat-near-isogenic lines in response to Puccinia striiformis tritici. *J Plant Interact* **20,** (2025).

44. Cai, X. & Qian, Q. Transcriptomic Insights into Wheat Disease Resistance. *Molecular Pathogens* (2024). doi:10.5376/mp.2024.15.0017

45. Mapuranga, J. *et al.* Harnessing genetic resistance to rusts in wheat and integrated rust management methods to develop more durable resistant cultivars. *Front Plant Sci* **13,** Preprint at https://doi.org/10.3389/fpls.2022.951095 (2022)

46. Gil, J. F. *et al.* Comparative Transcriptome Analysis Provides Molecular Insights into the Interaction of Beet necrotic yellow vein virus and Beet soil-borne mosaic virus with Their Host Sugar Beet. *Viruses* **12,** (2020).

47. Fan, H. *et al.* Transcriptome analysis of beta macrocarpa and identification of differentially expressed transcripts in response to beet necrotic yellow vein virus infection. *PLoS One* **10,** (2015).

48. Fan, H. *et al.* Deep sequencing-based transcriptome profiling reveals comprehensive insights into the responses of Nicotiana benthamiana to Beet necrotic yellow vein virus infections containing or lacking RNA4. *PLoS One* **9,** (2014).

49. Kanehisa, M. et al. KEGG: biological systems database as a model of the real world. Nucleic Acids Res **53**, (2025).

Competing interests: The authors declare no conflict of interest.

Funding: This study was supported by Embrapa (02.16.04.037.00.00), FAPESC (2024TR002600; 2023TR332), and CNPq (304883/2025-5; 309062/2021-7). S.C.N. and F.S.P. are Brazilian Federation for Support and Evaluation of Graduate Education (CAPES) fellows. F.N.S. receive CNPq fellowship.

Data availability statement: The datasets generated and analysed during the current study are available in the EMBL-EBI repository, https://www.ebi.ac.uk/biostudies/studies/S-BSST2255

Author contributions: Conceptualization: SCN, DL, and FNS; Methodology: SCN, FSP, GCM, DL, EEM, and FNS; Formal analysis and investigation: SCN, FSP, VIAS, VMS, ANJ, and PFG; Writing - original draft preparation: SCN, DL, and FNS; Writing – review, and editing: GCM, DL, EEM, and FNS; Funding acquisition: DL and FNS; Resources: DL and FNS; Supervision: DL and FNS. All authors critically revised the manuscript and approved of the final version.

Figure 1. (A) Disease symptoms in each tested wheat genotype. (B) The virus copy number obtained for each wheat genotype by qPCR. Two-way ANOVA and Tukey’s multiple comparison tests were applied to detect the statistical significance of the WhSMV titer in infected

Embrapa16 (a resistant genotype) and BRS Guamirim (a susceptible genotype), where *= $p < 0.05$.

Figure 2. (A) A bar chart showing the number of differentially expressed genes (DEGs) in the two genotypes after WhSMV infection. (B) A Venn diagram showing the total DEGs and their overlaps between two genotypes following WhSMV infection.

Figure 3. Treemap representation of the top Gene Ontology (GO) terms associated with differentially expressed genes (DEGs) across all comparisons. Each block represents a GO term, and its size is proportional to the number of associated DEGs. GO terms are colored by category: Biological Process (green), Cellular Component (orange), and Molecular Function (blue).

Figure 4. Comparative Gene Ontology (GO) enrichment analysis of differentially expressed genes in wheat genotypes following wheat stripe mosaic virus (WhSMV) infection. **(1)** Enriched GO terms for the resistant genotype Embrapa 16, comparing non-infected (E16C) and WhSMV-infected plants (E16S). **(2)** Enriched GO terms for the susceptible genotype BRS Guamirim, comparing non-infected (GuaC) and WhSMV-infected plants (GuaS). In each genotype, panel **(a)** shows enriched GO terms among down-regulated genes, and panel **(b)** shows enriched GO terms among up-regulated genes. GO terms are grouped by category: Biological Process (green), Cellular Component (orange), and Molecular Function (blue). Bars represent the number of genes

associated with each GO term. Asterisks (*) indicate significantly enriched terms (Fisher's exact test, adjusted p-value < 0.05).

Figure 5. KEGG schematic representation of the plant–pathogen interaction pathway (ko04626), highlighting key genes upregulated in Embrapa 16 under WhSMV infection, including PR1, WRKY33, RPM1, NBS-LRR, and CML16 [49].

Figure 6. Comparative analysis of plant-related pathways enriched in wheat genotypes infected with WhSMV. (A) Bubble plots depict metabolic and signaling pathways mapped through KEGG and Plant Reactome databases for the resistant genotype (E16C vs E16S) and the susceptible genotype (GuaC vs GuaS). (B) Bubble size represents the number of differentially expressed genes (DEGs) associated with each pathway. Colors indicate the functional category: defense (orchid), signal transduction (gold), hormone metabolism (coral), secondary metabolism (sky blue), photosynthesis (green), and lipid metabolism (sandy brown). Pathways marked with an asterisk (*) are significantly enriched (adjusted $p\text{-value} < 0.05$).

Figure 7. RT-qPCR analyses of six WhSMV infection-related genes in WhSMV-infected and non-infected (A) Embrapa 16 and (B) BRS Guamirim genotypes. Each bar represents the mean ± SEM of triplicate assays. T Test, Holm-Šídák method (* = $p < 0.05$).

A

B

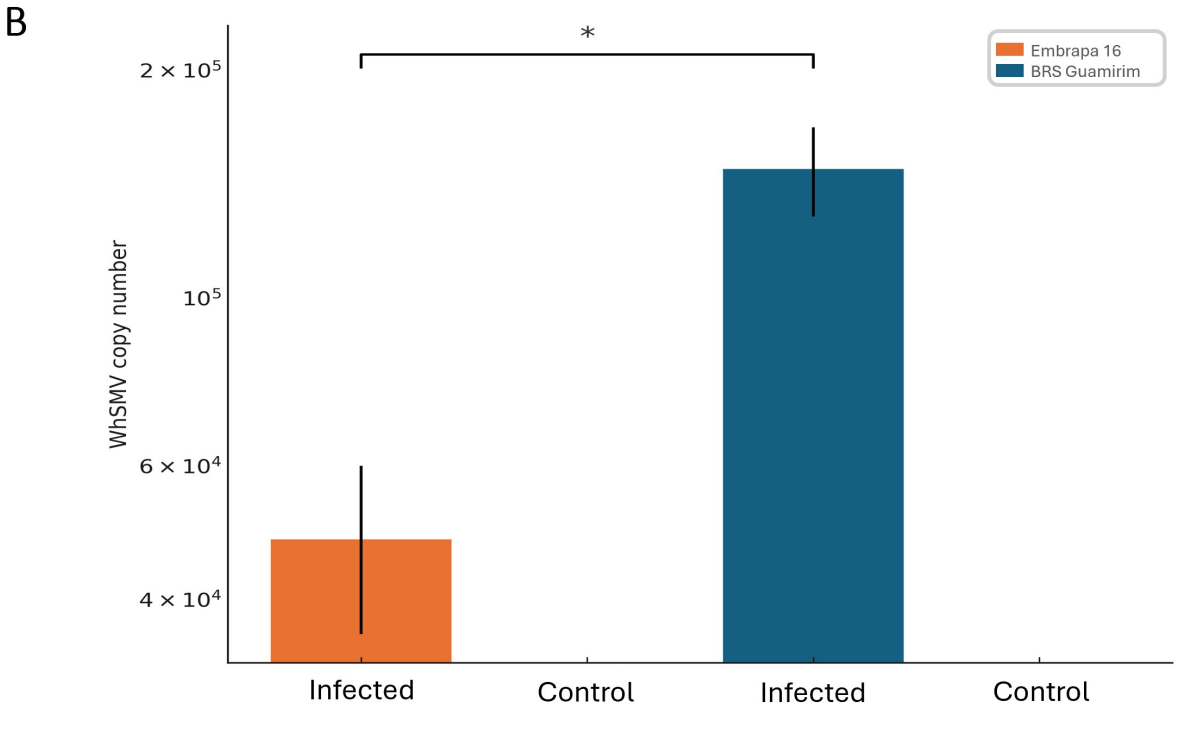

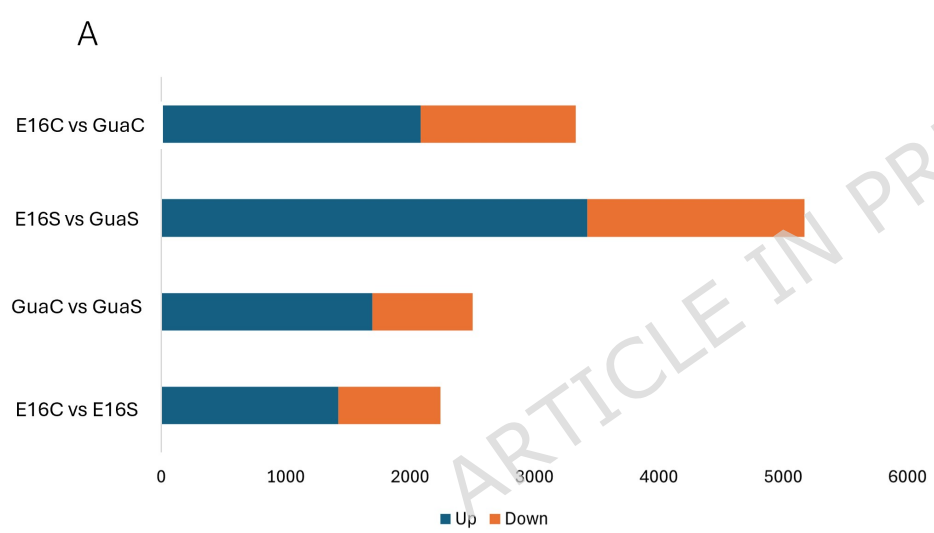

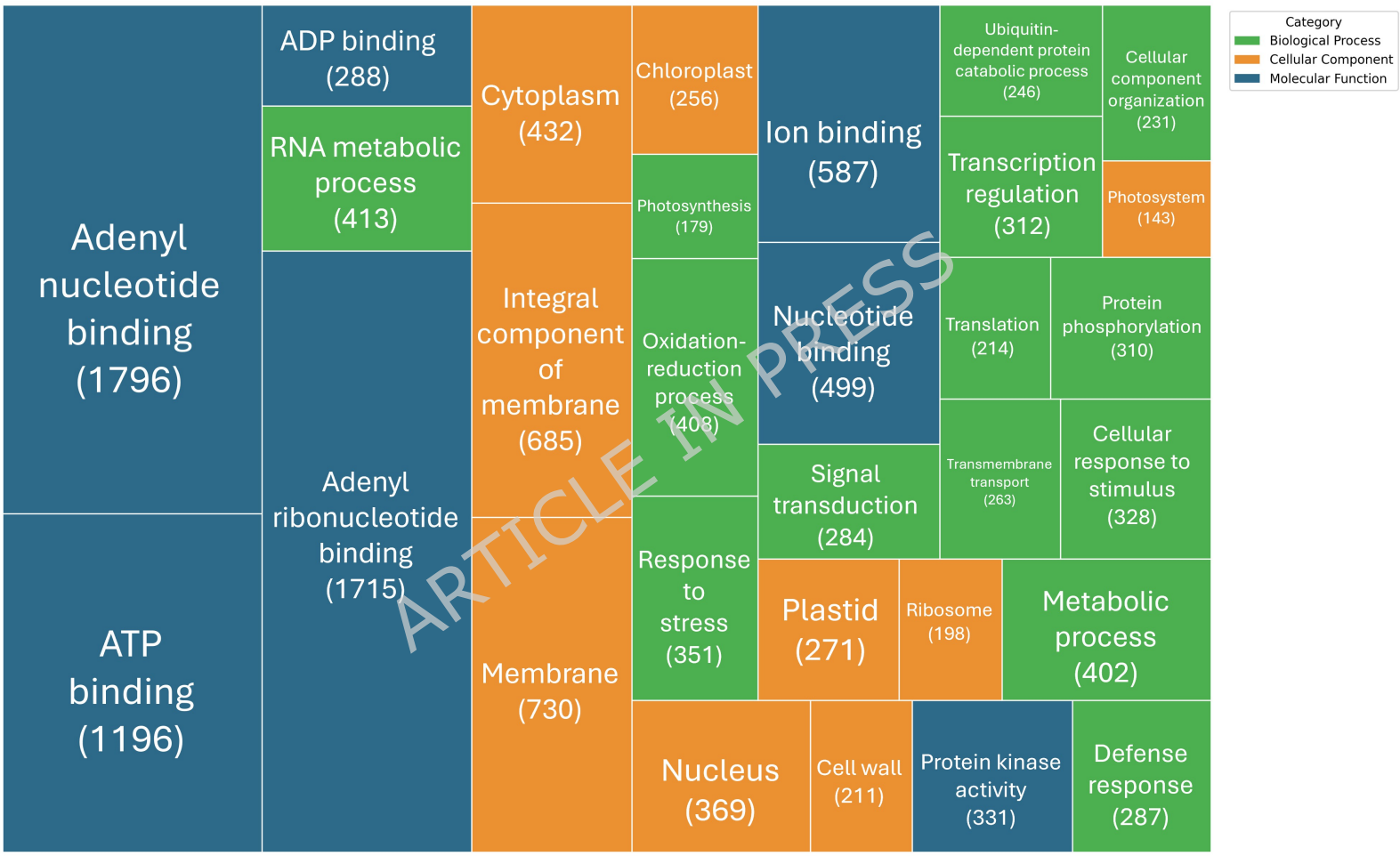

(1)

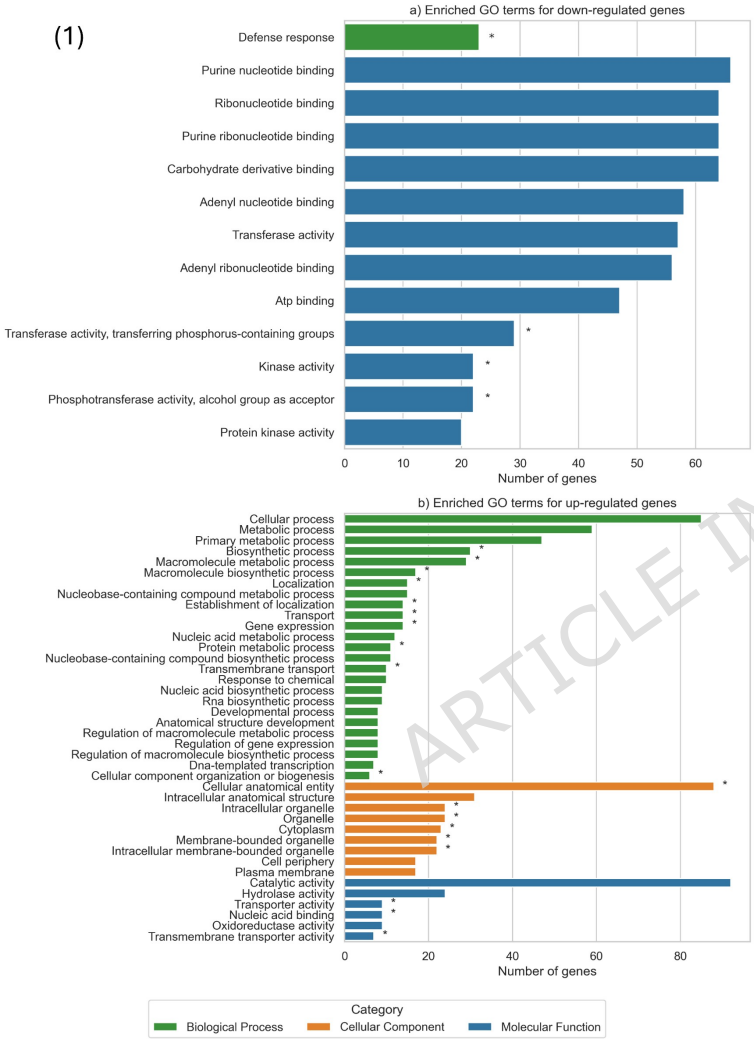

(2)

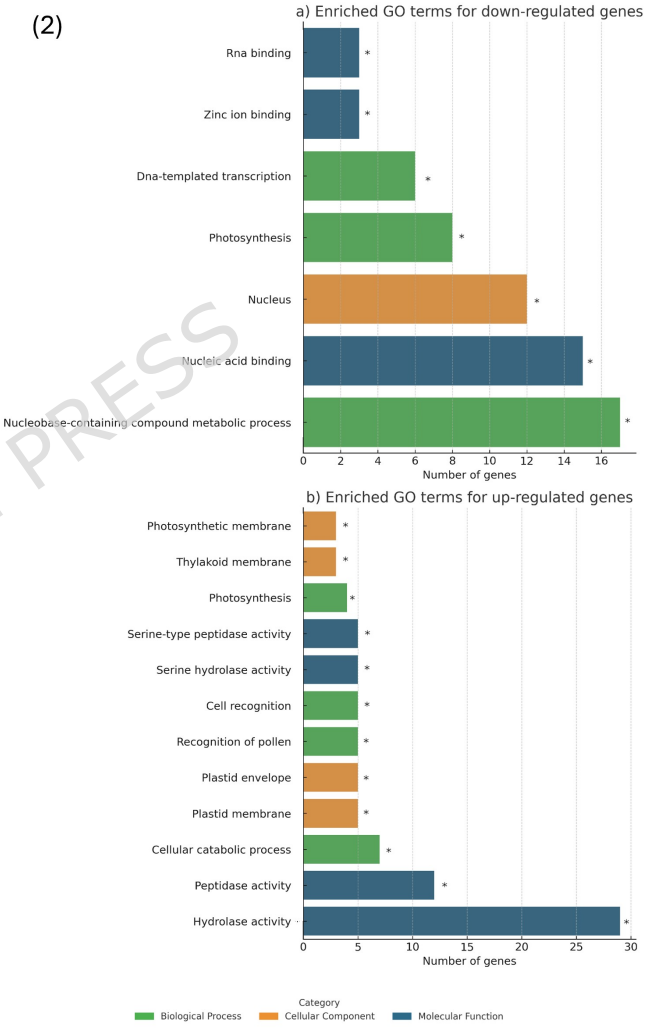

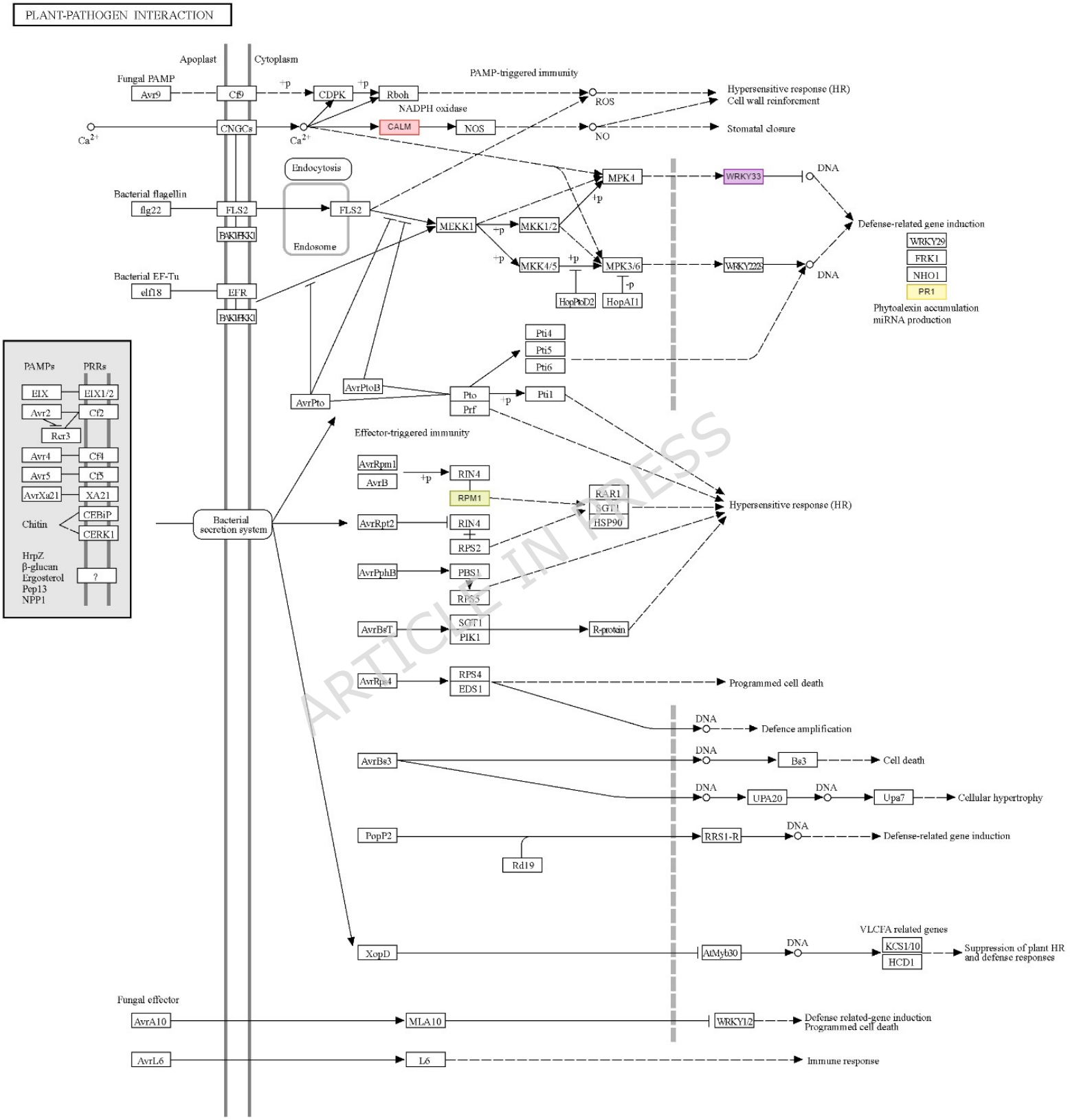

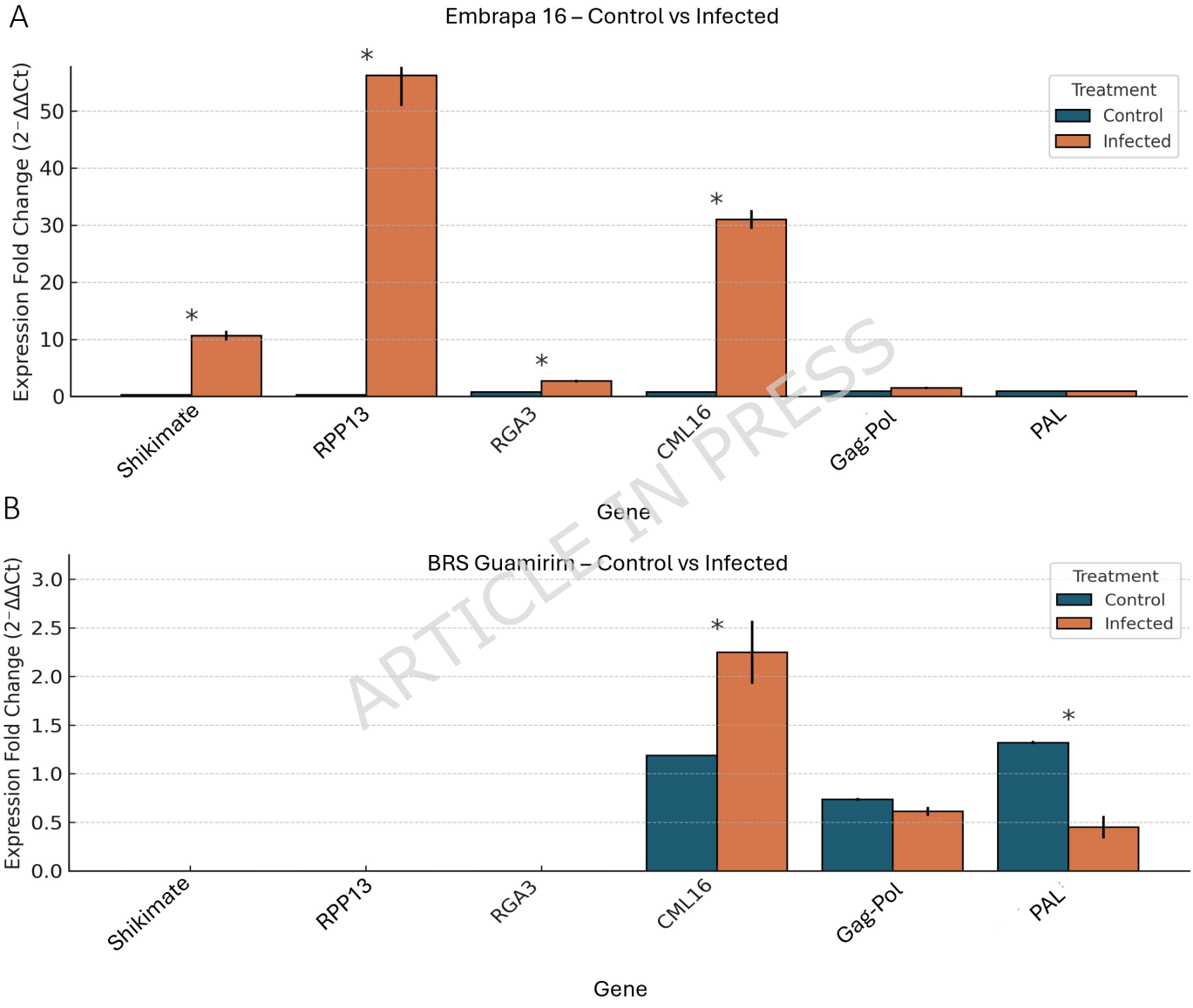

A

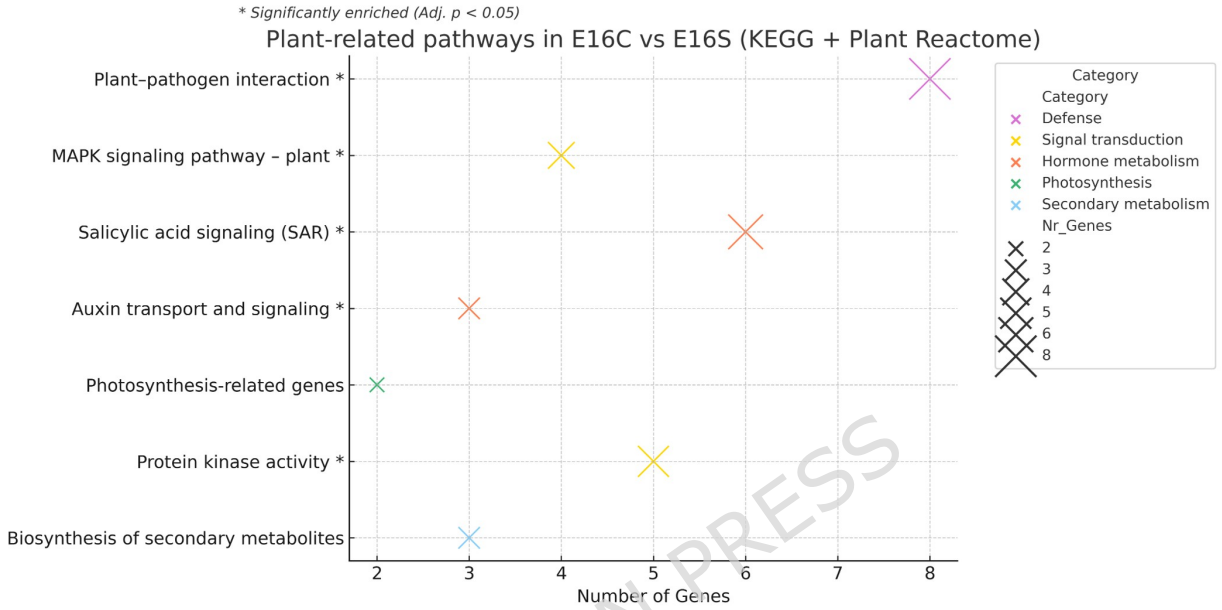

B